# Initial Analysis of Opponent-Colour Interactions Revealed in Sharpened Field Spectral Sensitivities

*DAVID H. FOSTER and ROSEMARY S. SNELGAR*

Field spectral sensitivities of the long- and medium-wavelength sensitive colour mechanisms of the human eye, when derived in the presence of a small, monochromatic (or white) auxiliary conditioning field, spatially coincident with the test field, are found (Foster, 1979, 1981) to be narrower and sharper than the corresponding Stiles Π mechanisms (Stiles, 1978). The peak of the long-wavelength sensitive mechanism shifts from about 570 nm to about 610 nm, and the peak of the medium-wavelength sensitive mechanism shifts from about 540 nm to about 530 nm. A shoulder or subsidiary lobe is also present on the short-wavelength side of the field spectral sensitivity (FSS) curve of the long-wavelength sensitive mechanism and a complementary though smaller shoulder is present on the long-wavelength side of the medium-wavelength sensitive mechanism. The short-wavelength sensitive mechanism shows no sharpening of its FSS curve with introduction of the coincident auxiliary field (at least for medium-to-high intensities of the field) (Foster, 1981). Evidence has been offered elsewhere that spectral sharpening of the long- and medium-wavelength sensitive mechanisms is the result of a shift from detection mediated by the non-opponent system to detection mediated by the opponent-colour system (Foster, 1981). It was hypothesized that the auxiliary field produces high spatial-frequency masking at the boundaries of the test and auxiliary fields; the spatial transient that would normally be responded to by the non-opponent system is suppressed.

COLOUR VISION
ISBN 0 12 000000 0

A fundamental question relating to the notion that opponent-colour interactions underlie spectral sharpening is this: can sharpened FSSs be represented as a simple difference of sensitivities of long- and medium-wavelength sensitive receptor mechanisms? To answer this question, we obtained data on spectral sharpening of FSSs of long- and medium-wavelength sensitive mechanisms over a range of intensities of a (monochromatic) auxiliary conditioning field, spatially coincident with the test field. To provide a set of fundamental mechanism sensitivities, we obtained (for the same subjects) unsharpened FSSs for the long-, medium-, and short-wavelength sensitive mechanisms, Stiles's mechanisms $\Pi_5$, $\Pi_4$, and $\Pi_3$ (or $\Pi_1$). A computer-based interactive modelling technique was then used to explore possible combinations of variously transformed sensitivities of long-, medium-, and short-wavelength sensitive fundamental mechanisms.

## Methods

Measurements were made using apparatus and methods described by Foster (1981), where details are given in full.

### *Field Spectral Sensitivity Measurements*

The test flash was monochromatic, disc-shaped, dia. 1.05° and of duration 200 msec. It was presented on a concentric disc-shaped, variable-intensity, monochromatic, main conditioning field, dia. 10.0°. The monochromatic auxiliary conditioning field, when present, was also disc-shaped and spatially coincident with the test field. A 3° square fixation array of four tiny lights was used to assist central fixation. Field spectral sensitivities were obtained by a direct field-adjustment method (Foster, 1981). The test flash of wavelength appropriate to the mechanism of interest was set 0.3 log units above increment (or absolute) threshold; the 10.0° main conditioning field was introduced, and its intensity adjusted by the subject to return the test flash to threshold. The efficiency and accuracy of this technique have been discussed elsewhere (Foster, 1981). Test-flash wavelengths were set at 664, 516, and 421 nm for the long-, medium-, and short-wavelength sensitive mechanisms respectively. For measurements of unsharpened FSSs, the coincident auxiliary field was removed. For the short-wavelength sensitive mechanism, however, a 10.0° 576-nm auxiliary field, intensity 9.31 log quanta $sec^{-1}$ $deg^{-2}$, was introduced to improve isolation of the mechanism (Stiles, 1978). To control for macular-pigment absorption on measured spectral sensitivities, the unsharpened FSS of the medium-wavelength sensitive mechanism was redetermined at 8° eccentricity. For measurements of sharpened FSSs, the coincident auxiliary field was set at 531 and 619 nm for the long- and medium-wavelength sensitive mechanisms respectively. Intensities of the auxiliary field were varied from 7.5 to 9.5 log quanta $sec^{-1}$ $deg^{-2}$.



Data presented here were obtained for subject JT, who was male, aged 20 years, had normal colour vision, and was unaware of the purpose of the experiment. Similar data were obtained from two other subjects.

### *Analysis*

Data on FSSs were analysed by means of a computer-based generalized linear interactive modelling technique GLIM (Baker and Nelder, 1978), with normal error and identity link. For completeness, a contribution from the short-wavelength sensitive fundamental mechanism was also included. Modelling was performed at two levels: immediately before and immediately after $\log_{10}$ compression of mechanism (quantum) sensitivity (compare Sperling and Harwerth, 1971; Ingling and Tsou, 1977; King-Smith and Kranda, 1981). The family of models thus under consideration at each level was as follows:

$$\begin{aligned} L'_I(\lambda) &= a_{I,L',L}L(\lambda) + a_{I,L',M}M(\lambda) + a_{I,L',S}S(\lambda) \\ M'_I(\lambda) &= a_{I,M',L}L(\lambda) + a_{I,M',M}M(\lambda) + a_{I,M',S}S(\lambda) \end{aligned} \qquad (1)$$

where:

$L$, $M$, and $S$ are the FSSs of the fundamental long-, medium-, and short-wavelength sensitive mechanisms,
$L'_I$ and $M'_I$ are the sharpened forms of $L$ and $M$ at auxiliary-field intensity $I$,
$\lambda$ is main-field wavelength,
$a_{I,j,k}$ are the coefficients weighting the $L$, $M$, and $S$ terms.

Note that for each auxiliary-field intensity $I$ and sharpened FSS the number of freely adjustable parameters was at most three. (A single additive constant relating absolute vertical positions of experimental and theoretical FSSs was subsumed.)

Smoothed versions of the fundamental functions L and M were used in Equations (1). This was not critical to the analysis and the smoothed and unsmoothed versions of the two fundamental functions did not differ by more than 0.027 log units RMSE over the affected portion of the wavelength range.

For each sharpened FSS $L'_I$ and $M'_I$ and auxiliary-field intensity $I$, maximum-likelihood estimators for the coefficients $a_{I,j,k}$ were computed by GLIM under various constraints, which included setting some coefficients to unity or zero.

Goodness of fit was evaluated generally by the unit-independent quantity $(w^2)'$, the proportion of variance *not* accounted for by the model (i.e., the ratio of variance about the predicted values to variance about the grand mean). For log-transformed spectral sensitivities, goodness of fit was also evaluated by RMSE, in log units.

## Results

In Fig. 1, unsharpened field spectral sensitivities for the long-, medium-, and short-wavelength sensitive mechanisms are shown by points indicated by open squares, circles, and diamonds, respectively. For ease of comparison, data for the short-wavelength sensitive mechanism have been displaced upwards by 1.0 log unit, and those for the medium-wavelength sensitive mechanism downwards by 0.2 log unit. The smooth curves joining the experimental points are cubic splines, and have no theoretical significance here.

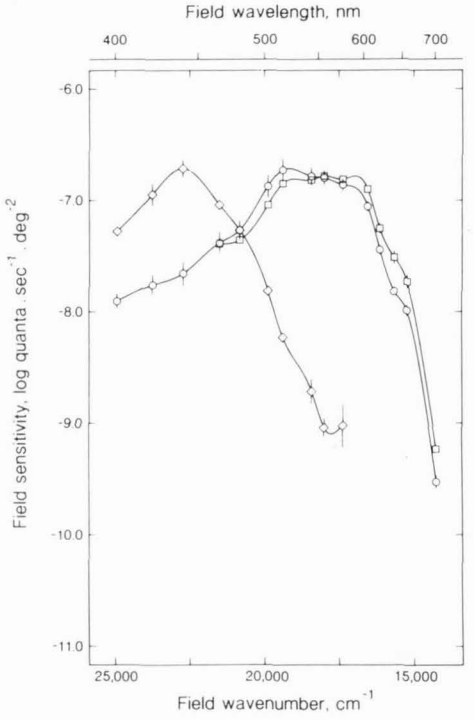


FIG. 1 Field spectral sensitivities of long-, medium-, and short-wavelength sensitive mechanisms (points indicated by open squares, circles, and diamonds respectively) determined without an auxiliary field coincident with the test field. The reciprocal of the intensity of a 10.0° main conditioning field necessary to raise test-flash threshold by 0.3 log units is plotted against the wavenumber of the main field. Data for the short-wavelength sensitive mechanism have been displaced upwards by 1.0 log unit and those for the medium-wavelength sensitive mechanism downwards by 0.2 log unit. For test-flash wavelengths, see text. Each point is the mean of either six or 12 readings and the vertical bars show ± 1 SEM where this is sufficiently large. Subject JT. (Smoothed versions of these data were used as fundamentals to generate the computer-fitted sharpened field spectral sensitivities shown in Figs 2a and b.)



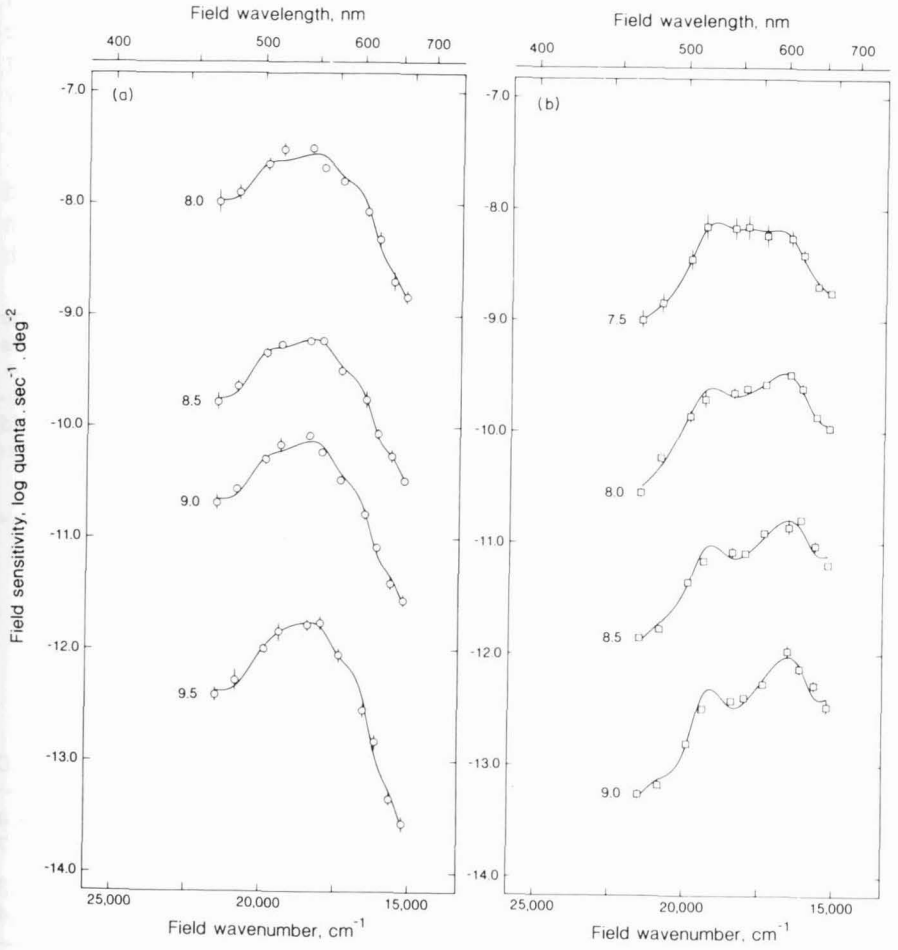


FIG. 2 (a) Field spectral sensitivities of the medium-wavelength sensitive mechanism determined with an auxiliary conditioning field, wavelength 619 nm, coincident with the test field. The reciprocal of the intensity of a 10.0° main conditioning field necessary to raise test-flash increment threshold by 0.3 log unit is plotted against main-field wavenumber. The intensity, in log quanta sec$^{-1}$ deg$^{-2}$, of the coincident auxiliary field is shown against each set of data. The top set of data is in the correct position. Each successive set has been displaced downwards by 1.0-log-unit increments. Each point is the mean of either six or 12 readings and the vertical bars indicate ± 1 SEM where this is sufficiently large. Subject JT. The smooth curves result from the best-fitting model (see text).

(b) Field spectral sensitivities of the long-wavelength sensitive mechanism determined with an auxiliary conditioning field, wavelength 531 nm, coincident with the test field. Other details as for Fig. 2a.

The open symbols in Figs 2a and 2b show FSSs for (2a) the medium-wavelength sensitive mechanism and (2b) the long-wavelength sensitive mechanism when obtained with an auxiliary field coincident with the test field. The intensity of the auxiliary field, in log quanta $sec^{-1}$ $deg^{-2}$, is indicated against each set of data. The top FSS in each figure is in the correct position; for clarity successive FSSs have been displaced downwards by 1.0-log-unit increments. The smooth curves in each figure result from the best-fitting model (see below).

Table 1 summarizes the results of the modelling. The quantity tabulated is $(w^2)'$, the proportion (per cent) of variance not accounted for by each model in fitting the sharpened FSSs of the long- and medium-wavelength

TABLE 1 Fits to the sharpened FSS data of Figs 2a and b (open symbols) of the two best-fitting models at pre-and post-log compression levels. "$L + M$" denotes the model $a_{l,j,L}L + a_{l,j,M}M$, and "$L + M + S$" the model $a_{l,j,L}L + a_{l,j,M}M + a_{l,j,S}S, j = L', M'$, see Equations (1). The proportion (per cent) of variance not accounted for $(w^2)'$ is shown for each of the models, levels, and auxiliary-field intensities. Significant reductions in $(w^2)'$ resulting from inclusion of short-wavelength component $S$ are indicated by * ($P < 0.001$).

| | | Sharpened FSS, medium-wavelength sensitive mechanism | | | | Sharpened FSS, long-wavelength sensitive mechanism | | | |
|---|---|---|---|---|---|---|---|---|---|
| | | Auxiliary-field intensity (log quanta $sec^{-1}$ $deg^{-2}$) | | | | Auxiliary-field intensity (log quanta $sec^{-1}$ $deg^{-2}$) | | | |
| | | 8.0 | 8.5 | 9.0 | 9.5 | 7.5 | 8.0 | 8.5 | 9.0 |
| pre-log level | "$L + M$" | 7.5 | 2.8 | 5.5 | 3.3 | 2.9 | 5.2 | 11.0 | 10.4 |
| | "$L + M + S$" | 6.9 | 1.5 | 4.3 | 1.7 | 0.8* | 5.2 | 10.2 | 9.7 |
| post-log level | "$L + M$" | 2.2 | 2.1 | 2.1 | 1.1 | 3.2 | 2.1 | 4.5 | 5.3 |
| | "$L + M + S$" | 1.8 | 0.3* | 1.0 | 0.9 | 0.6* | 1.8 | 3.4 | 2.4 |

sensitive mechanisms, at four different intensities of the auxiliary fields. Data are given for the two possible interaction levels (before and after log compression of mechanism sensitivity), and for the two most successful combinations of FSSs in each case (weighted combinations of FSSs of long- and medium-wavelength sensitive fundamental mechanisms, and of long-, medium-, and short-wavelength sensitive fundamental mechanisms).

Two points are evident. First, independent of the number of FSSs involved in the linear combinations, the fits at the post-log-compression level are uniformly better than at the pre-log-compression level. The total proportion of variance unaccounted for at the post-log level is 0.30–0.44 times smaller than at the pre-log level. In the case of the combination of three signals, this



reduction in variance unaccounted for is significant ($t_{14} = 2.56$, $P < 0.05$). Second, although there is the expected reduction in $(w^2)'$ with introduction of the short-wavelength sensitive mechanism (a consequence of an increase in the number of free coefficients in the model), the improvement in fit reaches significance only occasionally.

Table 2 lists for the sharpened FSSs of the long- and medium-wavelength sensitive mechanisms at the four auxiliary-field intensities the coefficients for

TABLE 2 Weighting coefficients (SEMs in parentheses) for the three-component log-transform model and RMSEs of each fit (without adjustment for individual degrees of freedom) to the experimental data of Figs 2a and b.

| | | Auxiliary-field intensity (log quanta $sec^{-1}$ $deg^{-2}$) | | | |
|---|---|---|---|---|---|
| | | 8.0 | 8.5 | 9.0 | 9.5 |
| Sharpened FSS, medium-wavelength sensitive mechanism | $a_{l,M',L}$ | −1.44(0.75) | −2.10(0.24) | −2.56(0.59) | −2.24(0.68) |
| | $a_{l,M',M}$ | 2.07(0.55) | 2.51(0.17) | 3.00(0.44) | 3.05(0.52) |
| | $a_{l,M',S}$ | −0.21(0.06) | −0.52(0.10) | −0.48(0.11) | −0.25(0.12) |
| RMSE (log units) | | 0.057 | 0.024 | 0.048 | 0.055 |
| | | Auxiliary-field intensity (log quanta $sec^{-1}$ $deg^{-2}$) | | | |
| | | 7.5 | 8.0 | 8.5 | 9.0 |
| Sharpened FSS, long-wavelength sensitive mechanism | $a_{l,L',L}$ | 0.60(0.30) | 2.33(0.42) | 3.05(0.78) | 3.92(0.79) |
| | $a_{l,L',M}$ | 0.04(0.22) | −1.47(0.31) | −2.21(0.57) | −2.88(0.58) |
| | $a_{l,L',S}$ | −0.29(0.02) | −0.14(0.15) | 0.09(0.11) | 0.35(0.10) |
| RMSE (log units) | | 0.023 | 0.041 | 0.061 | 0.061 |

the best-fitting model (three FSSs combined at the post-log-compression level). The quantities tabulated are the coefficients $a_{l,j,k}$ of Equations (1), along with their SEMs, and the RMSE, in log units, for each fit. There is a systematic increase in magnitude of the $L$ and $M$ coefficients with increase in auxiliary-field intensity $I$.

The smooth curves in Figs 2a and b respectively show, after spline interpolation, the results of the best-fitting model in relation to the sharpened FSSs of the medium- and long-wavelength sensitive mechanisms. Notice the systematic increase in magnitude of the lobe on the short-wavelength side of the long-wavelength sensitive mechanism as auxiliary-field intensity increases.

### *Adequacy of the Model*

How good is the fit of the three-component log-transform model specified in Table 2 to the experimental data? The total RMSE for the sharpened FSSs of the long- and medium-wavelength sensitive mechanisms over all auxiliary-field intensities is 0.048 log units; this rises to 0.067 log units when the number of degrees of freedom is taken into account. The latter RMSE may be compared with the experimentally measured SEM associated with individual data points of 0.060 log units. The difference is not significant ($F_{46,110} = 1.26$, $P > 0.1$).

## Discussion

The principal outcome of this analysis is that a simple weighted difference of sensitivities of long- and medium-wavelength sensitive fundamental mechanisms describes well the sharpened field spectral sensitivities of the long- and medium-wavelength sensitive mechanisms obtained when an auxiliary field is made coincident with the test field. For all the models specified in Table 1, the proportion of variance accounted for (the complement of $(w^2)'$) fell within the range 94.4–98.6 per cent. The fit was significantly better when carried out at the post-log-compression level than at the pre-log-compression level. The introduction of the short-wavelength sensitive mechanism led to a small, but not significant overall ($\chi^2_{64} \leq 12.6$, $P > 0.5$), improvement in fit.

An important qualitative attribute of the computed spectral sensitivities, mentioned earlier and illustrated in Figs 2a and b, is that there is an obvious lobe on the short-wavelength side of the sharpened FSSs for the long-wavelength sensitive mechanism, and a rather smaller effect for the medium-wavelength sensitive mechanism. This property of experimentally determined sharpened FSSs has been confirmed elsewhere (Foster and Snelgar, in prep).

The fact that model fitting was best at the post-log-compression level may have relevance to the observation that the SEMs associated with observed mean field sensitivities are essentially constant when measured in log quanta $sec^{-1}$ $deg^{-2}$.

Two caveats should be expressed concerning the representation here of sharpened FSSs of long- and medium-wavelength sensitive mechanisms as a simple weighted difference of fundamental spectral sensitivities evaluated after logarithmic compression. First, the operational FSSs of Fig. 2 are unlikely to represent solely the sensitivities of individual opponent-colour channels. For the adapting field probably acts to reduce sensitivity both at the receptors and at a later opponent site, and the relative strengths of these effects will vary with the wavelength of the main field. No attempt has been made in this initial analysis to disconfound these effects. Second, the compression of sensitivity by log transformation may be operationally indistinguishable from compression by some other plausible power-law functions.



## Acknowledgements

RSS was supported by an award from the Medical Research Council.

## References

Baker, R. J. and Nelder, J. A. (1978). *The GLIM System*. Algorithms Group, Oxford.

Foster, D. H. (1979). Effect of a small blue adapting field on the spectral sensitivity of the red-sensitive colour mechanism of the human eye. *Optica Acta* **26**, 293–296.

Foster, D. H. (1981). Changes in field spectral sensitivities of red-, green- and blue-sensitive colour mechanisms obtained on small background fields. *Vision Res.* **21**, 1433–1455.

Ingling, C. R., Jr and Tsou, B. H.-P. (1977). Orthogonal combinations of the three visual channels. *Vision Res.* **17**, 1075–1082.

King-Smith, P. E. and Kranda, K. (1981). Photopic adaptation in the red–green spectral range. *Vision Res.* **21**, 565–572.

Sperling, H. G. and Harwerth, R. S. (1971). Red–green cone interactions in the increment-threshold spectral sensitivity of primates. *Science* **172**, 180–184.

Stiles, W. S. (1978). *Mechanisms of Colour Vision*. London, Academic Press.

# Colour Vision

## *Physiology and psychophysics*

*Edited by*

J D Mollon
and
L T Sharpe

*The Psychological Laboratory*
*University of Cambridge*
*Cambridge, England*

1983

ACADEMIC PRESS
*A Subsidiary of Harcourt Brace Jovanovich, Publishers*

London New York
Paris San Diego San Francisco
São Paulo Sydney Tokyo Toronto